Single-ion effects in the formation of the heavy-fermion ground state in UBe_{13}

J. S. Kim, B. Andraka, C. S. Jee, S. B. Roy, and G. R. Stewart
Department of Physics, University of Florida, 215 Williamson Hall, Gainesville, Florida 32611-2085
(Received 27 November 1989)

We report a study of $U_{1-x}M_xBe_{13}$ ($0 \le x \le 0.995$ with the nonmagnetic M = Hf, Zr, Sc, Lu, Y, Pr, Ce, Th, and La), with characterization by x-ray diffraction, resistivity, dc susceptibility, and specific heat. Hybridization, and the distance, between the U $5f$ electrons and the Be s and p electrons is found to control the specific heat γ and therefore the effective mass m^*, while the outer electronic configuration of M plays no role. When the UBe_{13} lattice is not expanded by the dopant M, γ (normalized per U mole) reaches a constant value for $x > 0.15$ that is about 40% that of pure UBe_{13}. This dilute single-ion behavior is also observed in the resistivity. Surprisingly, the low-temperature magnetic susceptibility (normalized per U mole) is independent of doping for all x. Thus, the large magnetic susceptibility at low temperature in UBe_{13} is entirely attributable to single-ion effects. The source of the remaining 60% of the large m^* in UBe_{13} and the implications for heavy-fermion superconductivity are discussed.

I. INTRODUCTION

The source of the high effective mass m^* in heavy-fermion systems remains an important question.[1] $CePb_3$, which is magnetically ordered at 1.1 K, has been studied[2] down to $Ce_{0.1}La_{0.9}Pb_3$, with χ and C above 1.4 K exhibiting total independence of Ce concentration. Also, $Ce_{1-x}La_xCu_6$ has been studied[3] down to 10% Ce, with the result that the specific heat at low temperatures was observed to increase 40%. We report here a study of the properties of $U_{1-x}M_xBe_{13}$ ($0 \le x \le 0.995$) with the use of nine different M which, for the first time, provides clear experimental insight into the source of the heavy-fermion ground state in a uranium heavy-fermion system.

For such an ambitious undertaking, the design of the experiment is important. Potential problems to avoid in this initial study included: (1) The occurrence of magnetism at low temperatures and the associated large entropies obscuring the correct value for γ ($\equiv C/T$ as $T \to 0) \propto m^*$. This problem prevents the use of, e.g. $U_{1-x}M_xPt_3$, for this study, due to the ready occurrence of magnetism upon doping[4] in this material in the temperature regime, $T < 10$ K, where the heavy-fermion ground state forms. (2) Dealing with a host heavy-fermion system whose properties are irreproducible or difficult to reproduce, e.g., the peritectic formation of $CeAl_3$ with the known magnetic second phases of Ce_3Al_{11} and $CeAl_2$ involved[5] or the sensitivity of γ and magnetic susceptibility χ to Cu stoichiometry in $CeCu_2Si_2$.[6] (3) In choosing a heavy-fermion system UB_yC_z (or CeB_yC_z), a full range of solubility of M in the structure is important, or else the desired dilution of the f-atom cannot be achieved. Also, it is desirable that a number of MB_yC_z compounds should form, so that different M dilutant atoms may be used to investigate the effects of the M atoms, both due to its electronic configuration and its size, on the properties observed in $U_{1-x}M_xB_yC_z$ (or $Ce_{1-x}M_xB_yC_z$).

A heavy-fermion system that meets all three criteria is UBe_{13}. Ignoring highly radioactive elements (Pm,Am,Cm, . . .), twenty-six MBe_{13} compounds form in addition to UBe_{13}, providing a wide range of atoms M with the required unlimited intersolubility. Seventeen of

TABLE I. Properties of MBe_{13} Compounds. An asterisk denotes an unknown value.

M	a_0 (Å)	$T_{Néel}$ (K)
Hf	10.005	
Zr	10.043	
Sb	10.046	
Sc	10.102	
Mg	10.166	
Lu	10.173	
Yb	10.182	1.1
Tm	10.199	<0.45
Er	10.210	2.37
Ho	10.225	5.45
Np	10.226	3.4
Dy	10.233	9.3
Y	10.238	
Tb	10.254	15.3
U	10.256	$T_c = 0.97$
Pa	10.261	*
Gd	10.280	25.7
Pu	10.284	
Eu	10.300	
Ca	10.312	
Sm	10.325	8.8
Pm	10.33	*
Nd	10.360	2.63
Pr	10.367	
Ce	10.376	
Th	10.395	
La	10.456	
Sr	10.457	

these form nonmagnetic $M\mathrm{Be}_{13}$ compounds. (We are also conducting a study into the effects of magnetic-ion doping on UBe_{13} which, due to the inherent complications, is still in progress.) As may be seen in Table I, these seventeen $M\mathrm{Be}_{13}$ compounds have a broad range of electronic character (including M atoms that are rare earths, actinides, and transition metals) as well as size (a $4\frac{1}{2}\%$ difference in lattice parameter a_0 between HfBe_{13} and LaBe_{13}). Finally, MBe_{13} compounds generally form only at the one stoichiometry (no change of lattice parameter to five significant figures was detected[7] between preparations having the nominal compositions $\mathrm{UBe}_{11.15}$ and $\mathrm{UBe}_{15.0}$), with no other $M\mathrm{Be}_x$ compounds forming.

Using then $\mathrm{U}_{1-x}M_x\mathrm{Be}_{13}$ as the focus, the current work tries to separate three *a priori* interconnected effects (the change of the effective U-U distance upon dilution, the change of the U-Be distance upon changing a_0 with varying M, and the effect of the electronic nature of M) on the properties of $\mathrm{U}_{1-x}M_x\mathrm{Be}_{13}$ in order to determine what part single-ion effects play in the formation of large m^* below 10 K in UBe_{13}.

II. EXPERIMENTAL

Samples were prepared by arc melting together U (99.9%), M (typically 99.99%), and 99.8% Brush Wellman Be in a purified Ar atmosphere. The Be used was always premelted separately to try to remove gaseous impurities. In pure UBe_{13}, we have found[8] small changes in superconducting transition temperature T_c, of $<10\%$ and in the size of the peak at 2.5 K in the specific heat upon using very high purity (99.999%) U and Be. In the work presented here, however, the measured properties are not sensitive to which purity U and Be are used.

$\mathrm{U}_{1-x}M_x\mathrm{Be}_{13}$ compounds present two difficulties in preparation. (1) Remelting twice to insure homogeneity requires extreme care in bringing the arc slowly (several minutes) and at low power up to the already formed bead to avoid having the sample fly apart into pieces due to thermal stresses. Occasionally, already twice melted beads will spontaneously break apart upon cooling. (2) Since the melting point of UBe_{13} is so high (2000 °C), Be vapor loss is unavoidable upon melting. With experience and uniformity in preparation, additional Be can be added in the beginning (a 6% excess allows for three meltings) to compensate for this loss. As will be seen in the following, the uniformity of our results on a large number of samples argues that our preparation techniques ensure adequate reproducibility.

All samples were characterized by x-ray diffraction. No second phases were observed. Well resolved higher angle a_1-a_2 doublets were observed in $\mathrm{U}_{1-x}\mathrm{Y}_x\mathrm{Be}_{13}$ where, as seen from Table I, the lattice parameter does not change significantly with x. However, in cases where a_0 of the endpoint $M\mathrm{Be}_{13}$ differs significantly from that of UBe_{13} (e.g., for M=Sc or La) the higher angle lines are broadened by about a factor of 2 with the a_2 line being a barely discernible shoulder. It is important to note that with a change in a_0, both d_{M-M} and $d_{\mathrm{U-Be}}$ change.[9-11] This change in $d_{\mathrm{U-Be}}$ will be important in discussing the results in the following because of the strong hybridization effects between U $5f$-electrons and Be s-p electrons that must be present to prevent the U $5f$ electrons from localizing.

Resistivity samples were cut with cross sections of $\frac{1}{4}$ mm^2 by several mm long. Since cracks are common in UBe_{13} arc-melted buttons, care was taken to examine the $\frac{1}{2}$-mm thick slabs after the first cut under a microscope so as to cut bars that avoided the cracks. Resistance measurements were made using a dc, four-wire method.

Susceptibility and magnetization versus field measurements were made on all samples using an automated SQUID magnetometer from Quantum Design.

Specific-heat measurements, primarily down to 1.05 K and in zero field (but occasionally down to 0.33 K and up to 12 T) were made on small mass (5–10 mg) pieces of each specimen using a time constant method technique.[12]

III. RESULTS

The calculation of the effective mass has been variously treated,[13-15] with the derived values for pure UBe_{13} being $192m_e$, $296m_e$, and $260m_e$, respectively. All three models assume a spherical Fermi surface. This, coupled with the wide range of derived values for m^*, indicates that only a very rough estimate is obtained. Two of the models[14,15] use relations where $m^* \propto \gamma$ (γ is defined as the limit of C/T as temperature approaches zero). The other model involves[13] $m^* \propto \gamma(\rho_{\max})^{3/4}$, where $\rho_{\max}$ is the maximum resistivity value versus temperature ($\sim$241 $\mu\Omega$ cm at 2.2 K in the present work for pure UBe_{13}). Due to the uncertainty in the models, complicated by the difficulty in separating the proper $\rho_{\max}$ in a disordered $\mathrm{U}_{1-x}M_x\mathrm{Be}_{13}$ system with a Nordheim disorder term present, we have chosen to simply present low-temperature specific-heat data γ values as being (roughly) proportional to m^*.

A. Resistivity

The resistivities between 1 and 300 K of six samples of $\mathrm{U}_{1-x}\mathrm{Y}_x\mathrm{Be}_{13}$, $x=0$, 0.035, 0.2, 0.9, and 1.0 are shown in Fig. 1, with expanded low-temperature plots for four samples of $\mathrm{U}_{1-x}\mathrm{Y}_x\mathrm{Be}_{13}$ with $x \leq 0.03$ shown in Fig. 2. The resistivities of $\mathrm{U}_{0.1}M_{0.9}\mathrm{Be}_{13}$ for M = Th, La, Sc, and Y between 1 and 300 K are shown in Fig. 3. Error bars for the data are $\pm 10\%$, primarily due to uncertainties in the cross-sectional area of the bar and in the voltage contact separation.

Possible additional errors would be due to undetected cracks giving too high a value for ρ. Our data, Fig. 1, appear to show a monotonic behavior of ρ versus doping, implying lack of undetected cracks. Also, small differences in Be stoichiometry between samples may affect the absolute values of resistivity obtained to some degree. We are not aware of any studies of the magnitude of ρ as a function of Be stoichoimetry variations. A preliminary study on our part on samples of $\mathrm{UBe}_{13.85}$ and $\mathrm{UBe}_{11.94}$ indicates a lowering of ρ for both concentrations as compared to that reported for pure UBe_{13}. For the stoichiometry variations present in our $\mathrm{U}_{1-x}M_x\mathrm{Be}_{13}$

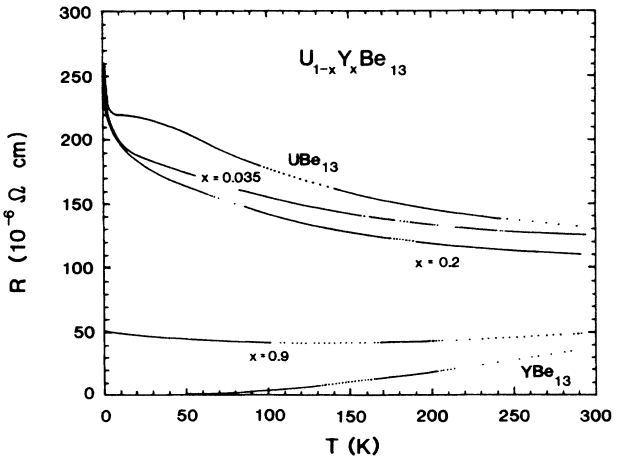

FIG. 1. Resistivity (accuracy ±10%) vs temperature for $U_{1-x}Y_xBe_{13}$. Clearly, the upturn seen in pure UBe_{13} continues even to 90% dilution by Y. It is also interesting to observe the evolution with doping of the flat plateau in ρ out to 25 K in pure UBe_{13}. It becomes a shoulder already in the resistivity of $U_{0.99}Y_{0.01}Be_{13}$ (not shown), becomes an even weaker shoulder in the resistivity of $U_{0.98}Y_{0.02}Be_{13}$, and is almost absent in the resistivity data for $U_{0.97}Y_{0.03}Be_{13}$, with the feature remaining at around 25 K for all three samples. The data shown here for $U_{0.965}Y_{0.035}Be_{13}$ show no evidence for this feature.

samples, any lowering of resistivity would be less than 10%, our geometrical factor error.

At the lowest temperatures, UBe_{13} has a peak in ρ versus T theorized[16] to be due to coherence between the

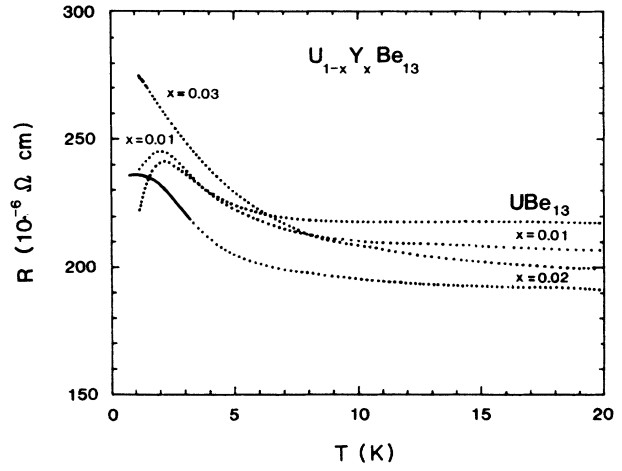

FIG. 2. Low-temperature resistivity (accuracy ±10%) of low doped $U_{1-x}Y_xBe_{13}$. The peak at 2.2 K in the data for pure UBe_{13} broadens and shifts slightly lower in temperature for $x=0.01$, and becomes a flat plateau extending from T_c (0.5 K) up to 1.7 K for $x=0.02$. The resistivity for $x=0.03$ rises above the value for pure UBe_{13} below 6 K and is 15% larger at 1.1 K. Since the room-temperature resistivity values for pure and $x=0.03$ $U_{1-x}Y_xBe_{13}$ agree fairly well as expected (see Fig. 1), this 15% difference at 1.1 K, although within the error limits, may be significant.

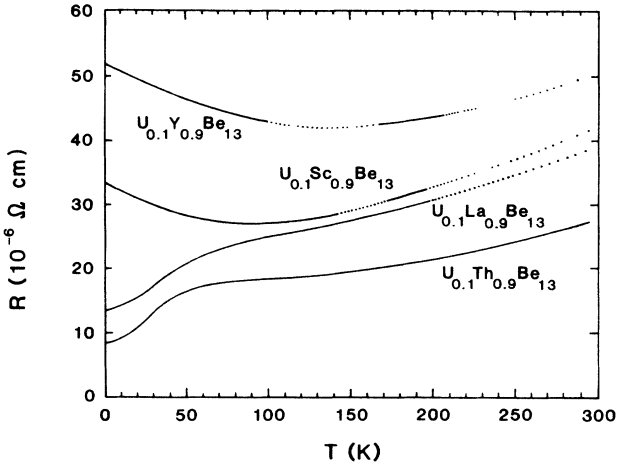

FIG. 3. Resistivity vs temperature for $U_{0.1}(Th,La,Sc,Y)_{0.9}Be_{13}$. An upturn in resistivity below 125 K for Y, and 80 K for Sc, doping is observed, with $\rho(T\rightarrow 0)$ much lower for the Sc doped sample. For La and Th doping, a shoulder at around 50 K is observed, as seen in pure UBe_{13}, Fig. 1.

U $5f$ scattering sites below 2.2 K with incoherent scattering at higher temperatures leading to the high absolute values observed. As small amounts of Y are added, Fig. 2 the "coherence" peak moves to lower temperatures as the doping introduces additional incoherent scattering [which also causes the increase in $\rho(T\rightarrow 0)$]. This same qualitative behavior for low Th doping has been previously observed.[17]

At higher temperatures, Fig. 1, we observe a decrease in the observed resistivity as x increases in $U_{1-x}Y_xBe_{13}$. However, still at $x=0.9$, or only 10% U, the resistivity remains quite high at low temperatures in comparison with the resistivity of pure YBe_{13}, with a characteristic

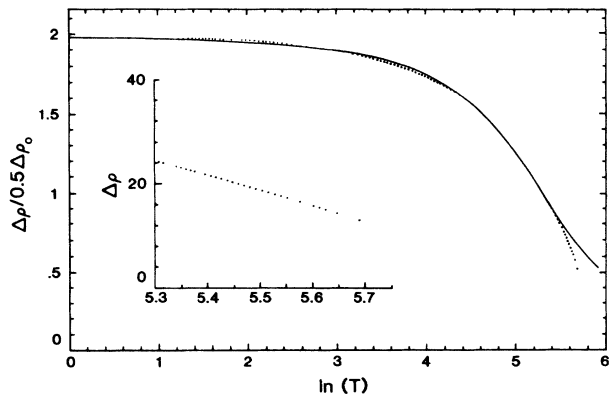

FIG. 4. $\Delta\rho=\rho(U_{0.1}Y_{0.9}Be_{13})-\rho(YBe_{13})$ divided by $\frac{1}{2}\Delta\rho(T\rightarrow 0)$ is plotted vs $\log_e T$ (points). The solid line is the fit from Ref. 18. The parameters obtained ($T_{Kondo}=195$ K, spin=0.13) are not very physical, since (Ref. 20) the model is really designed for transition metal Kondo systems. The inset shows $\Delta\rho$ vs $\log_e T$ at higher temperature.

"Kondo single-impurity" upturn in ρ below 150 K. Figure 4 shows the resistivity attributable just to the U ions

$$[\rho(U_{0.1}Y_{0.9}Be_{13})-\rho(YBe_{13})] \text{ vs } \ln T \ .$$

($[\rho(YBe_{13})]$ rather than $0.9\rho(YBe_{13})$ is used so as to subtract off the full phonon term. Also, no Nordheim disorder term, which is expected to be small and independent of temperature, is subtracted. Doing so does not affect the analysis materially.)

Although 10% U is clearly not yet in the dilute regime, the effective U-U distance is over twice as large as in pure UBe_{13}. Can we fit these ρ data in Fig. 4 with a Kondo model behavior? A model[18] developed for the *s-d* Kondo problem has been used to describe Ce (Ref. 19) and Sm (Ref. 20) systems, among others, up to concentrations similar to the 10% under discussion here. Crystal-field effects may[20] complicate the picture, since these are not treated by the model.[18] Figure 4 shows that this model fits our resistivity data rather well, although the fit parameters obtained ($T_{\text{Kondo}}=195$ K, spin $=0.13$), as expected[20] are not very physical. (As seen in the following, the higher temperature susceptibility data give an effective moment consistent with a larger value for the spin, while the low-temperature specific heat γ via

TABLE II. Magnetic Parameters for $U_{1-x}M_xBe_{13}$.

Sample	χ^a at $T=1.8$ K (10^{-3} emu/mole U)	μ_{eff} (μ_B/mole U)
UBe_{13}	15.1±0.2	3.08
$U_{0.95}Y_{0.05}Be_{13}$	16.1	3.31
$U_{0.8}Y_{0.2}Be_{13}$	14.7	
$U_{0.6}Y_{0.4}Be_{13}$	16.7	
$U_{0.4}Y_{0.6}Be_{13}$	13.6	
$U_{0.2}Y_{0.8}Be_{13}$	14.3	3.49
$U_{0.1}Y_{0.9}Be_{13}$	17.0	4.04
$U_{0.05}Y_{0.95}Be_{13}$	17.9	4.67–5.04
$U_{0.026}Y_{0.974}Be_{13}$	12.8	
$U_{0.01}Y_{0.99}Be_{13}$	16.6	
YBe_{13}	0.32 (per mole YBe_{13})	
$U_{0.97}Sc_{0.03}Be_{13}$	13.6	
$U_{0.85}Sc_{0.15}Be_{13}$	13.2	
$U_{0.5}Sc_{0.5}Be_{13}$	12.0	
$U_{0.1}Sc_{0.9}Be_{13}$	12.6	3.9
$ScBe_{13}$	0.027 (per mole $ScBe_{13}$)	
$U_{0.97}La_{0.03}Be_{13}$	15.9	
$U_{0.85}La_{0.15}Be_{13}$	17.9	
$U_{0.5}La_{0.5}Be_{13}$	15.8	
$U_{0.1}La_{0.9}Be_{13}$	16.2	3.29
$LaBe_{13}$	−0.26 (per mole $LaBe_{13}$)	
$U_{0.85}Th_{0.15}Be_{13}$	16.27	
$U_{0.69}Th_{0.31}Be_{13}$	15.2	
$U_{0.53}Th_{0.47}Be_{13}$	16.1	
$U_{0.1}Th_{0.9}Be_{13}$	16.0	3.27
$ThBe_{13}$	0.090 (per mole $ThBe_{13}$)	
$U_{0.1}Pr_{0.9}Be_{13}$	20.4	
$PrBe_{13}$	45.3	
$U_{0.9}Ce_{0.1}Be_{13}$	15.6	
$U_{0.85}Ce_{0.15}Be_{13}$	15.8	
$U_{0.1}Ce_{0.9}Be_{13}$	12.3	3.07
$CeBe_{13}$	1.87 (per $CeBe_{13}$ mole)	
$U_{0.85}Lu_{0.15}Be_{13}$	15.3	
$U_{0.1}Lu_{0.9}Be_{13}$	14.5	3.70
$LuBe_{13}$	0.46 (per $LuBe_{13}$ mole)	
$U_{0.1}Zr_{0.9}Be_{13}$	14.5	3.42
$ZrBe_{13}$	0.095 (per $ZrBe_{13}$ mole)	
$U_{0.1}Hf_{0.9}Be_{13}$	12.4	3.53
$HfBe_{13}$	−0.014 (per $HfBe_{13}$ mole)	

[a] $x\chi(MBe_{13})$ at 1.8 K is subtracted from χ^{measured} and the resulting difference is divided by $(1-x)$ to give χ per mole U.

$T_{\text{Kondo}} \propto 1/\gamma$ gives $T_{\text{Kondo}} \approx 20$ K.) At higher temperatures, the data fit a simple $\ln T$ dependence as shown in the inset to Fig. 4. Thus, our $U_{0.1}Y_{0.9}Be_{13}$ resistivity appears to, within the uncertainties of model[21–23] applicability and effect of crystal fields, behave as that for more classical Kondo systems.

The comparison between the resistivities of $U_{0.1}M_{0.9}Be_{13}$ for M=Y, Sc, La, and Th is shown in Fig. 3. Clearly, Sc and Y have a different low-temperature behavior in their resistivity than La and Th. The atoms with equal or smaller radii than that of U (Sc and Y) show a Kondo upturn in the resistivity at low temperatures, while the larger La (isoelectronic to Y and Sc) and Th show a more metallic behavior. Although further work would be required to confirm this trend, as will be seen in the following this is consistent with our other data.

B. Susceptibility

Unlike resistivity, *dc* susceptibility is relatively insensitive to minor amounts of either excess Be or excess U between grains of UBe_{13}. Thus, samples of $UBe_{12.6}$ and $UBe_{14.1}$ prepared intentionally off stoichiometry have susceptibilities equal to that (see Table II) found for stoichiometric UBe_{13} (within the 5–8% range of the stoichiometry variation), whereas resistivity, as we have shown in the preceding section, is more sensitive to stoichiometry.

The dc susceptibilities at the lowest temperatures of measurement 1.8 K, for our magnetometer for each $U_{1-x}M_xBe_{13}$ sample are shown in Table II. The Curie-Weiss law effective moments calculated from the straight-line behavior of χ^{-1} versus T between 100 and 400 K for the $U_{1-x}M_xBe_{13}$ samples of the present work are also shown in Table II. The value of χ(1.8 K) for a given $U_{1-x}M_xBe_{13}$ is normalized per U mole via

$$[\chi^{\text{measured}} - x\chi(M\text{Be}_{13})]/(1-x) .$$

This necessitated the preparation and characterization of the pure $M\text{Be}_{13}$ compounds as well. In order to calculate $\mu_{\text{effective}}$ per U mole, the appropriate $x\chi(M\text{Be}_{13})$ needs to be subtracted between 100 and 400 K. For low doping, this is a negligible correction. For large doping, i.e., for low U content, this involves taking the difference of two similarly sized numbers, the result of which is multiplied by the large factor $1/1-x$. Our magnetometer's accuracy is not sufficient to warrant this procedure for $x \geq 0.95$, due to the increasingly large error bars (see Table II).

Within these caveats, the data in Table II present a clear picture. The large magnetic susceptibility at low temperatures in nonmagnetically ordered heavy-fermion systems[5] is thought to be linked with the process by which local moments present at room temperature (as seen in the Curie-Weiss behavior of χ^{-1}) are compensated and prevented from ordering at lower temperatures. As may be immediately seen in Table II, this large low-temperature magnetic susceptibility in UBe_{13} appears to be *entirely due* to single-ion effects, i.e., independent of U concentration. Between $U_{0.95}Y_{0.05}Be_{13}$ and $U_{0.01}Y_{0.99}Be_{13}$, a total of nine differing x values gives an average χ (1.8 K) per U mole of 15.5×10^{-3} emu, i.e., essentially unchanged from that of pure UBe_{13}. For M isoelectronic with Y, i.e., Sc and La, either a slight decrease or increase respectively in χ (1.8 K)/U mole is observed. This effect may be linked to the change in U-Be distance in the case of Sc and La, with little change for Y, and will be discussed further with the specific-heat data presented in the following. The χ (1.8 K) results for the other $U_{1-x}M_xBe_{13}$ samples similarly show only rather small variations versus the value of 15.1 ± 0.2 memu/mole for pure UBe_{13}, with the exception of $U_{0.1}Pr_{0.9}Be_{13}$ which, based on the value for pure $PrBe_{13}$, may be approaching magnetism. (As seen in Table I, $PrBe_{13}$ is the rare earth, Be_{13}, which is the next largest in lattice parameter after the last magnetically ordered $R\text{Be}_{13}$ listed in the lattice-parameter-ordered table of properties.)

This result, that the large magnetic susceptibility observed at low temperature in UBe_{13} is essentially independent of U concentration is an important finding of the present work. As will be seen in the following the specific-heat data of $U_{1-x}M_xBe_{13}$, when coupled with the fact that $\chi_{\text{low } T} \neq f$(U concentration) in UBe_{13} has important implications for the mechanism that produces the high effective mass in UBe_{13}.

C. Specific heat

Specific heat is a bulk measurement and is quite insensitive to small variations in stoichiometry. The parameter of importance here is the specific heat γ ($\equiv C/T$ as $T\rightarrow0$), proportional to the effective mass m^* of the conduction electrons. As will be seen, the scatter in our γ values[24] expressed as per U mole will be relatively small ($\pm10\%$) which, due to the large scaling factors $1/(1-x)$ involved in the dilute samples, argues well for the homogeneity and accuracy of stoichiometry in our samples.

In pure UBe_{13}, C/T varies rapidly at low temperatures–rising a factor of 2 between 3 and 0.9 K, where superconductivity and the accompanying anomaly occurs. Upon doping,[7,25] with $\sim$3–5% M, superconductivity is suppressed. The specific heat divided by temperature for UBe_{13} and $U_{0.97}Y_{0.03}Be_{13}$ between 1.05 and 10 K is shown in Fig. 5. Upon further doping, C/T becomes even less temperature dependent (see Fig. 5), thus allowing us to present C/T data in the dilute limit (or even up to 90% U) taken down to 1.05 K on pumped[4] He as being representative of γ ($\equiv C/T$ as $T\rightarrow0$). This was confirmed in measurements on $U_{0.1}Sc_{0.9}Be_{13}$ down to 0.35 K - C/T is indeed only weakly temperature dependent for $x > 0.05$. Another complication in determining C/T in the concentrated limit in UBe_{13} is the peak in C at $\sim$2.5 K which shifts upon doping, but remains present up to 5–10% doping—thus affecting the value of C/T near the peak and necessitating lower-temperature measurements (0.3 or 0.1 K) to correctly determine γ and thus m^*. In the present work, we focus on the nonconcentrated regime, where the peak in C is no longer present.

As discussed in the Introduction, three different effects occur upon substitution for U in UBe_{13}: change in $d^{\text{eff}}_{\text{U-U}}$,

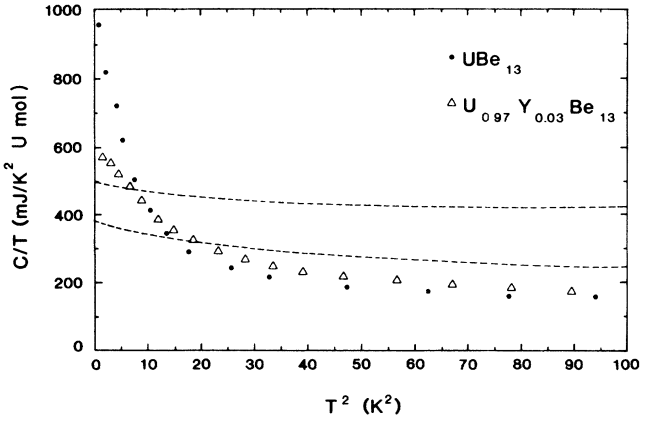

FIG. 5. Specific heat of pure UBe_{13} and $U_{0.97}Y_{0.03}Be_{13}$ divided by temperature vs temperature squared. The rapid ($\sim 30\%$) decrease in γ with such small amounts of doping is clear, with little change above 3 K. The C/T vs T^2 data for dilute, $0.1 \leq x \leq 0.995$, $U_{1-x}Y_xBe_{13}$ all lie within the envelope defined by the two dashed lines.

change in d_{U-Be}, and possible effects due to the differing electronic nature of M. Thus, to begin with, we present specific-heat γ values (at 1.05 K) versus composition for isoelectronic Sc, Y, and La in Fig. 6. Consider first the Y case, where a_0 (YBe_{13}) $\simeq a_0$ (UBe_{13}) (see Table I). In the regime $x < 20\%$, γ and m^* fall sharply with increasing doping. (The exact details of this fall are intertwined with the change of the peak in C with doping). However, for $0.20 \leq x \leq 0.995$, γ per U mole of $U_{1-x}Y_xBe_{13}$, with almost no scatter in the data, remains constant—independent of U concentration—at a value of 420±40 mJ/U mole K^2. (This early result of our work led to investigation of further, more closely interspersed Y compositions to confirm this as seen in Fig. 6.) The case of Sc, where a_0 ($ScBe_{13}$) $< a_0$ (UBe_{13}) (Table I), is similar to that of Y with the constant γ reached in the dilute limit more nearly 300 mJ/U mole K^2.

The case of La is different. γ does not fall as quickly with increasing x in the concentrated regime. More importantly, γ for $U_{1-x}La_xBe_{13}$ continues to fall monotonically even in the dilute limit.

In order to investigate this difference in γ versus x dependence for Sc and Y versus La, the specific-heat γ values of eleven other $U_{1-x}M_xBe_{13}$ samples in the nonconcentrated, $x \geq 0.15$ limit were measured. All the data are presented in Fig. 7. These data allow a number of conclusions. First, the electronic nature of M is apparently not significantly affecting γ of the remaining U ions in the lattice. For example, Ce, Pr, Th, and La have widely varying outer-shell electronic configurations, yet γ per U mole of $U_{0.1}M_{0.9}Be_{13}$ for these atoms is approximately the same.

Second, d^{eff}_{U-U} in this nonconcentrated regime does not appear to be the important variable for determining γ and m^*. As we saw for Sc and Y, M atoms with $a_0(MBe_{13}) \leq a_0$ (UBe_{13}), including Lu, Zr, and Hf as well as Sc and Y, have a γ per U mole almost independent of concentration as shown in Fig. 7. For these cases, γ is independent of d^{eff}_{U-U} for $x \geq 0.15$. For the cases where a_0 (MBe_{13}) $> a_0$ (UBe_{13}) (Ce, La, Th, and Pr), it could be argued that γ plotted versus d^{eff}_{U-U} would give a monotonic

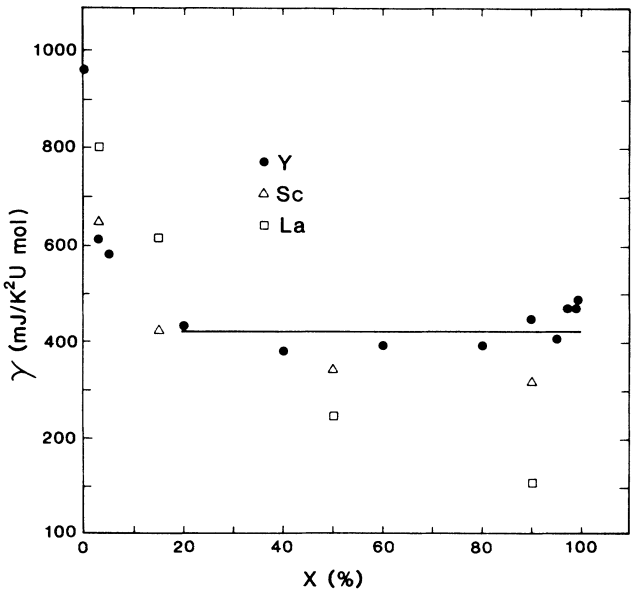

FIG. 6. Specific-heat γ values for $U_{1-x}M_xBe_{13}$, M = Y, Sc and La, vs doping level x. Sc and Y behave similarly, with a rapid decrease in γ with only a few percent doping (see Fig. 5 as well), followed by an approximately constant value for γ for $x \geq 0.15$. La, however, causes a smooth decrease of γ with increasing concentration with no plateau region reached.

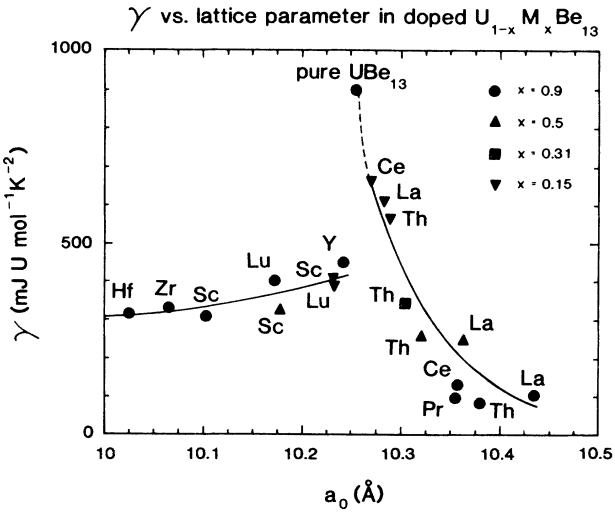

FIG. 7. Specific heat γ of 18 $U_{1-x}M_xBe_{13}$ samples vs lattice parameter in the nonconcentrated, $x \geq 0.15$ limit. As discussed in the text, for smaller MBe_{13} an essentially constant region of γ vs x is found as seen in Fig. 6 for Sc and Y. For larger dopant atoms M, e.g., La as shown in Fig. 6, γ falls monotonically with increasing a_0, independent of which metal M is used.

(albeit of very low slope for $x>0.5$) plot. However, atoms of essentially identical $d^{\text{eff}}_{\text{U-U}}$ from smaller a_0 group on the same plot would have much different γ values. Thus, $d^{\text{eff}}_{\text{U-U}}$ for $U_{0.1}Th_{0.9}Be_{13} \approx d^{\text{eff}}_{\text{U-U}}$ for $U_{0.1}Sc_{0.9}Be_{13} \approx 2.15 * d^{\text{pure UBe}_{13}}_{\text{U-U}} = 11$ Å, while the γ's are a factor of 3.6 different. However, when the data are plotted versus a_0 as shown in Fig. 7, which stresses $d_{\text{U-Be}}$ as the important parameter, γ varies smoothly with a_0.

Thus, it appears that it is the hybridization between the U $5f$ electrons and the Be s and p electrons, which depends critically upon separation, that dominates the behavior of γ per U mole upon dilution. If the U-Be separation remains the same as found in UBe_{13} (2.15 Å) or smaller, then the hybridization remains effective in the single-ion, U-concentration-independent mechanism that creates a γ per U mole of about 375 mJ/U mole K^2 or about 40% of that in pure UBe_{13}. For increases in the U-Be separation above that found in pure UBe_{13}, even in the 1–2% range, clearly the creation of this still large dilute-limit constant γ and accompanying m^* does not occur.

One way to check this hypothesis that $d_{\text{U-Be}}$ is the factor that determines γ in the nonconcentrated regime in $U_{1-x}M_xBe_{13}$ would be to mix two M atoms in a given sample to achieve a given a_0, and see if γ for this $U_{1-x}(M_1M_2)_xBe_{13}$ material has the γ expected from the plot shown in Fig. 7. Using the lattice parameter data shown in Table I, we have prepared and characterized $U_{0.1}La_{0.39}Sc_{0.51}Be_{13}$, expected to have a lattice parameter equal to that for UBe_{13}. X-ray diffraction on this sample reveals broadened high angle lines as expected due to a strain from the three varying-size atoms on the U site. The lattice parameter is, however, as predicted. $\chi(1.8\text{ K}) \simeq 18$ memu/U mole. The specific heat γ per U mole is 435 mJ/U mole K^2, compared with 450 mJ/U mole K^2 for $U_{0.1}Y_{0.9}Be_{13}$, which has essentially the same lattice parameter. This result nicely supports the hypothesis that $d_{\text{U-Be}}$ determines γ per U mole in $U_{1-x}M_xBe_{13}$ in the nonconcentrated regime.

What is the mechanism that creates the dilute limit γ of 450 mJ/U mole K^2 in $U_{0.005}Y_{0.995}Be_{13}$, Fig. 6, or, in general, the 375 ±75 mJ/U mole K^2 γ observed independent of x for $x \geq 0.15$ for those M atoms with a_0 (MBe$_{13}$) $\leq a_0$(UBe$_{13}$)? It is not very informative (although it is shown here for the first time) to say that the mechanism depends critically on $d_{\text{U-Be}}$. The one model thought to be valid for Ce systems in the dilute limit is of course the Kondo model. We have seen above that the resistivity of $U_{0.1}Y_{0.9}Be_{13}$ has Kondo-like behavior.

The specific heat of dilute Kondo impurities can be calculated.[26] Figure 8 shows the (unrenormalized, unadjusted) C/T data below 10 K for YBe_{13}, $U_{0.005}Y_{0.995}Be_{13}$, and $U_{0.05}Y_{0.95}Be_{13}$. The slope β of a C/T vs T^2 plot ($C/T=\gamma+\beta T^2$) for a normal metal is inversely proportional to the Debye temperature, a measure of the lattice stiffness, via

$$\theta_D = \left[\frac{1944(r)}{\beta(\text{mJ/mole K}^4)}\right]^{1/3} \times 10 ,$$

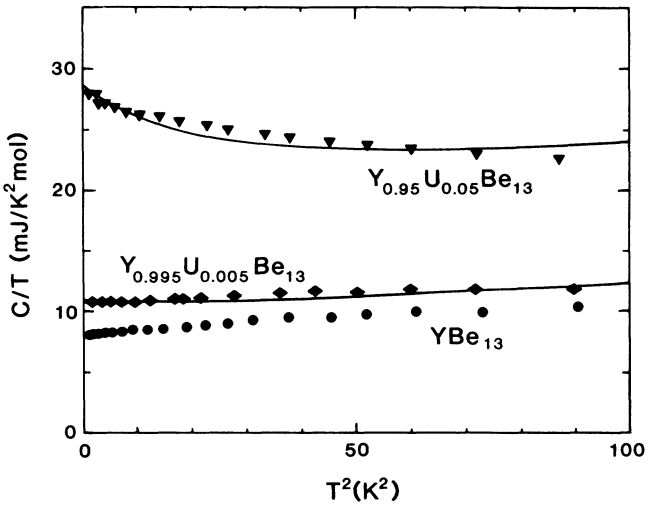

FIG. 8. Specific heat divided by temperature vs temperature squared for two dilute limit $U_{1-x}Y_xBe_{13}$ samples and pure YBe_{13}. The solid lines are fit to the single-ion Kondo model of Ref. 26. The parameters obtained from the fits are the following: for $x=0.995$, $T_K=22$ K, $\gamma=9$ mJ/mole K^2, and $\theta_D=1000$ K; for $x=0.95$, $T_K=23$ K, $\gamma=9.8$ mJ/mole K^2, and $\theta_D=750$ K.

where r is the number of atoms in the formula unit, i.e., 14 here.

For YBe_{13}, the low-temperature data in Fig. 8 give $\theta_D=970$ K. This high value is expected due to the large amount of Be (whose $\theta_D=1480K$) (Ref. 27 reports $\theta_D=820$ K for $LaBe_{13}$, 930±20 K for $LuBe_{13}$, and 618 K for $ThBe_{13}$.) As may be seen from Fig. 8, as U is added to YBe_{13}, the heavy-fermion upturn in C/T occurs at low temperatures, obscuring the simple determination of θ_D. However, a fit may be made to the C/T data for $U_{0.005}Y_{0.995}Be_{13}$ and $U_{0.05}Y_{0.95}Be_{13}$, using the model of Ref. 26. The result of this fitting procedure ($C/T=C_{\text{Kondo}}/T+\gamma+\beta T^2$) is shown in Fig. 8. The fit, unlike the resistivity model discussed above, should apply to f-electron systems and is being used at low enough temperatures to avoid crystal-field level complications. The Kondo temperature ($\equiv T_K$), γ, and β terms obtained and listed in the caption to Fig. 8 are not too unrealistic. In particular, the value of θ_D obtained from β (1000 K) for $x=0.995$ is quite close to the value of 970 K obtained from the pure YBe_{13} data. No credence should be attached to either the value itself for T_K or its lack of change with composition, as the scatter in the data limit the accuracy of T_K.

IV. DISCUSSION

It is remarkable that the specific-heat confirmation of the continued presence of heavy electron, large-γ behavior in dilute $U_{1-x}Y_xBe_{13}$ and $U_{1-x}Sc_xBe_{13}$, and of more normal metallic behavior in dilute $U_{1-x}La_xBe_{13}$ and $U_{1-x}Th_xBe_{13}$ is mirrored by the behavior of the resistivity (Fig. 3)—Kondo upturn and remaining large ρ_0 for

M=Y and Sc, with a more metallic resistivity for M=La and Th. Second, γ is smooth, monotonic, and single valued for all $U_{1-x}M_xBe_{13}$ ($x \geq 0.15$) samples when plotted (Fig. 7) versus a_0, $\propto d_{U-Be}$. This, coupled with the γ result of $U_{0.1}La_{0.39}Sc_{0.51}Be_{13}$ being predictable from a_0, is a strong argument for U-5f-electron hybridization with Be s and p electrons being central to whatever single-ion mechanism is responsible for the dilute limit $\gamma \sim 40\%$ $\gamma_{UBe_{13}}$ found for all $U_{1-x}M_xBe_{13}$ with $a_0 \leq a_0$ (UBe_{13}), independent of U concentration. [Since the other limited studies[2,3] of dilution ($x > 0.5$) effects in heavy-fermion systems are exclusively in Ce systems with an M (La) slightly larger in size than Ce, comparison of the present results to other systems must await further work.]

It is further noteworthy that $\chi(U_{1-x}M_xBe_{13})$, where magnetic MBe_{13} are avoided, is within narrow limits of scatter independent of U concentration for *all* x, from pure UBe_{13} to $U_{0.005}Y_{0.995}Be_{13}$ and for all M. Thus, the mechanism that creates this large χ=15 memu/mole in pure UBe_{13} (a factor of 20 times that of Pd, the most strongly enhanced element) is also *purely* a single-ion effect. Therefore, the present work suggests a focus for further work—what is responsible for the correlation effect in the concentrated U regime ($x < 0.10$) that creates the remaining 60% of the γ and m^* observed in pure UBe_{13}? Is this correlation effect intimately connected to the occurrence of superconductivity in UBe_{13}? After all, it is this correlation mechanism that causes the low χ/γ value in UBe_{13}—long identified[5,28] as the only known common feature unique to the three heavy-fermion superconductors $CeCu_2Si_2$, UBe_{13}, and UPt_3.

ACKNOWLEDGMENTS

This work was performed at the University of Florida under U.S. Department of Energy Contract No. DE-FG05-86ER45268. The authors would like to thank T.H. Geballe, F. Steglich, A.L. Giorgi, and P. Kumar for helpful discussions.

[1]See, for example, theoretical papers in the Proceedings of the 6th International Conference on Crystal Field Effects and Heavy Fermion Physics [J. Magn. Magn. Mater. **76&77** (1988)].

[2]C. L. Lin, A. Wallash, J. E. Crow, T. Mihalisin, and P. Schlottmann, Phys. Rev. Lett. **58**, 1232 (1987).

[3]K. Satoh, M. Kato, Y. Maeno, T. Fujita, Y. Onuki, and T. Komatsubara, Jpn. J. Appl. Phys. **26**, 521 (1987); K. Satoh, T. Fujita, Y. Maeno, Y. Onuki, and T. Komatsubara, J. Magn. Magn. Mater. **76&77**, 128 (1988).

[4]G. R. Stewart, A. L. Giorgi, J. O. Willis, and J. O'Rourke, Phys. Rev. B **34**, 4269 (1986).

[5]G. R. Stewart, Rev. Mod. Phys. **56**, 755 (1984).

[6]B. Batlogg, J. P. Remeika, A. S. Cooper, G. R. Stewart, Z. Fisk, and J. O. Willis, J. Magn. Magn. Mater. **47&48**, 42 (1985).

[7]J. L. Smith, Z. Fisk, J. O. Willis, A. L. Giorgi, R. B. Roof, H. R. Ott, H. Rudigier, and E. Felder, Physica **135B**, 3 (1985).

[8]C. S. Jee, B. Andraka, J. S. Kim, S. Roy, and G. R. Stewart (unpublished).

[9]XAFS work on other pseudobinary solid solutions ($Ga_{1-x}In_xAs$[10] and $K_{1-x}Rb_xBr$[11]) has shown that the nearest-neighbor distances are significantly different from that inferred from a simple Vegard's law linear extrapolation between the a_0's of the endpoints. Thus, although the calculated lattice parameters of our $U_{1-x}M_xBe_{13}$ samples [$a_0 = a_0(UBe_{13}) + x*(a_0(MBe_{13}) - a_0(UBe_{13}))$] agree quite well with that derived from the x-ray diffraction peak positions the XAFS results imply that a certain strain should exist in the lattice due to the mismatch in U-Be nearest-neighbor distance with adjacent M-Be nearest-neighbor distance. (The XAFS experiments find that the cation-cation distances—in our case the U-M atoms—do follow Vegard's law, as observed in our lattice parameter versus x behavior.) This quantitative difference in the U-Be distance from a linear Vegard's law extrapolation, although expected (Refs. 10 and 11) to be significant, does not alter the qualitative fact that the U-Be separation changes upon doping with a different-sized cation.

[10]J. C. Mikkelsen, Jr. and J. B. Boyce, Phys. Rev. B **28**, 7130 (1983).

[11]J. B. Boyce and J. C. Mikkelsen, Jr., Phys. Rev. B **31**, 6903 (1985).

[12]G. R. Stewart, Rev. Sci. Instrum. **54**, 1 (1983).

[13]H. R. Ott, H. Rudigier, Z. Fisk, and J. L. Smith, Phys. Rev. Lett. **50**, 1595 (1983).

[14]M. B. Maple, J. W. Chen, S. E. Lambert, Z. Fisk, J. L. Smith, H. R. Ott, J. S. Brooks, and M. J. Naughton, Phys. Rev. Lett. **54**, 477 (1985).

[15]U. Rauchschwalbe, Physica B+C **147**, 1 (1987).

[16]For a recent review of this, see N. Grewe and F. Steglich, in *Heavy Fermions,* Vol. 14 of *Handbook of Physics and Chemistry of Rare Earths,* edited by K. Gschneidner, Jr. and L. Eyring (North-Holland, Amsterdam, in press), Chap. 97.

[17]J. L. Smith, Z. Fisk, J. O. Willis, B. Batlogg, and H. R. Ott, J. Appl. Phys. **55**, 1996 (1984).

[18]D. R. Hamann, Phys. Rev. **158**, 570 (1967); P. E. Bloomfield and D. R. Hamann, Phys. Rev. **164**, 856 (1967).

[19]A. Najib, J. Pierre, M. J. Besnus, P. Haen, A. P. Murani, and E. Siaud, J. Magn. Magn. Mater. **76&77**, 135 (1988).

[20]S. Bakanowski, J. E. Crow, and T. Mihalisin, Solid State Commun. **22**, 241 (1977).

[21]An attempt to fit our data to the (presumably more applicable) model developed for Ce compounds in Ref. 22 fails due to the presence of a maximum in the fit from the crystal-field splitting inferred (Ref. 23) from specific heat rather than a shoulder as observed in pure UBe_{13}. Thus, despite the significantly larger number of parameters in this second model, (Ref. 22) it fails to fit the shape of the resistivity measured for our UBe_{13} and $U_{1-x}M_xBe_{13}$ samples.

[22]Y. Lassailly, A. K. Bhattacharjee, and B. Coqblin, Phys. Rev. B **31**, 7424 (1985).

[23]R. Felten, F. Steglich, G. Weber, H. Rietschel, F. Gompf, B. Renker, and J. Beuers, Europhys. Lett. **2**, 323 (1986).

[24]The specific-heat γ values are normalized as were the χ (1.8 K) values above by subtracting $x\gamma(MBe_{13})$. However, except for $CeBe_{13}$, where γ=71 mJ/mole K^2, the γ values of pure MBe_{13} are only about 8 mJ/mole K^2. Thus this normalization is a minor correction except for very dilute, large-x $U_{1-x}M_xBe_{13}$ samples. Also, the precision of our specific-heat

apparatus is approximately 1%, making the subtraction of, e.g., $0.995\gamma(YBe_{13})$ ($=8.15$ mJ/mole K^2) from $\gamma(U_{0.005}Y_{0.995}Be_{13})$ ($=10.6$ mJ/mole K^2) a fairly accurate procedure.

[25]E. Zirngiebl, J. D. Thompson, J. L. Smith, and Z. Fisk, *Theoretical and Experimental Aspects of Valence Fluctuations and Heavy Fermions,* edited by L. C. Gupta and S. K. Malik (Plenum, New York, 1987), p. 349.

[26]K. D. Schotte and U. Schotte, Phys. Lett. **55A**, 38 (1975).

[27]E. Bucher, J. P. Maita, G. W. Hull, R. C. Fulton, and A. S. Cooper, Phys. Rev. B **11**, 440 (1975).

[28]Z. Fisk, H. R. Ott, and G. Aeppli, Jpn. J. Appl. Phys. **26**, 1882 (1987).